Year: 2012

Transplantation and tracking of human-induced pluripotent stem cells in a pig model of myocardial infarction: assessment of cell survival, engraftment, and distribution by hybrid single photon emission computed tomography/computed tomography of sodium iodide symporter transgene expression

Templin, Christian ; Zweigerdt, Robert ; Schwanke, Kristin ; Olmer, Ruth ; Ghadri, Jelena-Rima ; Emmert, Maximilian Y ; Müller, Ennio ; Küest, Silke M ; Cohrs, Susan ; Schibli, Roger ; Kronen, Peter W ; Hilbe, Monika ; Reinisch, Andreas ; Strunk, Dirk ; Haverich, Axel ; Hoerstrup, Simon ; Lüscher, Thomas F ; Kaufmann, Philipp A ; Landmesser, Ulf ; Martin, Ulrich

Abstract: BACKGROUND: Evaluation of novel cellular therapies in large-animal models and patients is currently hampered by the lack of imaging approaches that allow for long-term monitoring of viable transplanted cells. In this study, sodium iodide symporter (NIS) transgene imaging was evaluated as an approach to follow in vivo survival, engraftment, and distribution of human-induced pluripotent stem cell (hiPSC) derivatives in a pig model of myocardial infarction. METHODS AND RESULTS: Transgenic hiPSC lines stably expressing a fluorescent reporter and NIS (NIS(pos)-hiPSCs) were established. Iodide uptake, efflux, and viability of NIS(pos)-hiPSCs were assessed in vitro. Ten (±2) days after induction of myocardial infarction by transient occlusion of the left anterior descending artery, catheter-based intramyocardial injection of NIS(pos)-hiPSCs guided by 3-dimensional NOGA mapping was performed. Dual-isotope single photon emission computed tomographic/computed tomographic imaging was applied with the use of (123)I to follow donor cell survival and distribution and with the use of (99m)TC-tetrofosmin for perfusion imaging. In vitro, iodide uptake in NIS(pos)-hiPSCs was increased 100-fold above that of nontransgenic controls. In vivo, viable NIS(pos)-hiPSCs could be visualized for up to 15 weeks. Immunohistochemistry demonstrated that hiPSC-derived endothelial cells contributed to vascularization. Up to 12 to 15 weeks after transplantation, no teratomas were detected. CONCLUSIONS: This study describes for the first time the feasibility of repeated long-term in vivo imaging of viability and tissue distribution of cellular grafts in large animals. Moreover, this is the first report demonstrating vascular differentiation and long-term engraftment of hiPSCs in a large-animal model of myocardial infarction. NIS(pos)-hiPSCs represent a valuable tool to monitor and improve current cellular treatment strategies in clinically relevant animal models.

DOI: https://doi.org/10.1161/CIRCULATIONAHA.111.087684

Templin, Christian; Zweigerdt, Robert; Schwanke, Kristin; Olmer, Ruth; Ghadri, Jelena-Rima; Emmert, Maximilian Y; Müller, Ennio; Küest, Silke M; Cohrs, Susan; Schibli, Roger; Kronen, Peter W; Hilbe, Monika; Reinisch, Andreas; Strunk, Dirk; Haverich, Axel; Hoerstrup, Simon; Lüscher, Thomas F; Kaufmann, Philipp A; Landmesser, Ulf; Martin, Ulrich (2012). Transplantation and tracking of human-induced pluripotent stem cells in a pig model of myocardial infarction: assessment of cell survival, engraftment, and distribution by hybrid single photon emission computed tomography/computed tomography of sodium iodide symporter transgene expression. Circulation, 126(4):430-439.
DOI: https://doi.org/10.1161/CIRCULATIONAHA.111.087684

Circulation

Circulation

Transplantation and Tracking of Human Induced Pluripotent Stem Cells in a Pig Model of Myocardial Infarction: Assessment of Cell Survival, Engraftment and Distribution by Hybrid SPECT-CT Imaging of Sodium Iodide Symporter Trangene Expression

Christian Templin, Robert Zweigerdt, Kristin Schwanke, Ruth Olmer, Jelena R. Ghadri, Maximillian Emmert, Ennio Müller, Silke M. Küest, Susan Cohrs, Roger Schibli, Peter Kronen, Monika Hilbe, Andreas Reinisch, Dirk Strunk, Axel Haverich, Simon Hoerstrup, Thomas F. Luescher, Philipp A. Kaufmann, Ulf Landmesser, and Ulrich Martin

CIRCULATIONAHA/2011/087684 [R2]

Author Disclosures

Christian Templin:
Research Grant: Swiss Life Foundation, Amount: >= $10,000
Gottfried and Julia Bangerter-Rhyner-Foundation, Amount: >= $10,000
Swiss National Foundation, Amount: >= $10,000

Robert Zweigerdt: No disclosures

Kristin Schwanke: No disclosures

Ruth Olmer: No disclosures

Jelena R. Ghadri: No disclosures

Maximillian Emmert: No disclosures

Ennio Müller: No disclosures

Silke M. Küest: No disclosures

Susan Cohrs: No disclosures

Roger Schibli: No disclosures

Peter Kronen: No disclosures

Monika Hilbe: No disclosures

Andreas Reinisch: No disclosures

Dirk Strunk:
Research Grant: Austrian Research Fund NAN-N211, Amount: >= $10,000

Axel Haverich: No disclosures

Simon Hoerstrup: No disclosures

Thomas F. Luescher: No disclosures

Philipp A. Kaufmann:
Research Grant: Swiss National Foundation, Amount: >= $10,000

Ulf Landmesser:
Research Grant: Swiss National Foundation, Amount: >= $10,000

Ulrich Martin: No disclosures

Transplantation and Tracking of Human Induced Pluripotent Stem Cells in a Pig Model of Myocardial Infarction: Assessment of Cell Survival, Engraftment and Distribution by Hybrid SPECT-CT Imaging of Sodium Iodide Symporter Trangene Expression

Running title: Templin – Long term *in vivo* imaging of iPSCs in pig hearts

Christian Templin[1,2#], MD; Robert Zweigerdt[2], PhD; Kristin Schwanke[2], PhD; Ruth Olmer[2], PhD; Jelena-Rima Ghadri[3], MD; Maximilian Y. Emmert[4], MD; Ennio Müller[3]; Silke M. Küest[3], MD; Susan Cohrs[5], PhD; Roger Schibli[5], PhD; Peter Kronen[6,7,8], DVM; Monika Hilbe[9], DVM; Andreas Reinisch[10], MD, PhD; Dirk Strunk[10], MD; Axel Haverich[2], MD; Simon Hoerstrup[4], MD, PhD; Thomas F. Lüscher[1], MD; Philipp A. Kaufmann[3], MD; Ulf Landmesser[1]*, MD; Ulrich Martin[2*#], PhD

[1]Cardiovascular Center, Cardiology, University Hospital Zurich, Switzerland
[2]Leibniz Research Laboratories for Biotechnology and Artifical Organs, Cardiothoracic, Transplantation and Vascular Surgery, Hannover Medical School, Germany
[3]Cardiovascular Center, Cardiac Imaging, University Hospital Zurich, Switzerland
[4]Clinic for Cardiovascular Surgery, Department of Surgical Research, University Hospital Zurich, Switzerland
[5]Center for Radiopharmaceutical Science ETH-PSI-USZ, Paul Scherrer Institute, Villigen, Switzerland
[6]Veterinary Anaesthesia Services – International, Winterthur, Switzerland
[7]Center for Applied Biotechnology and Molecular Medicine (CABMM), Vetsuisse Faculty, University of Zurich, Switzerland
[8]Musculoskeletal Research Unit, Equine Department, Vetsuisse Faculty ZH, University of Zurich, Switzerland
[9]Institute of Veterinary Pathology, Vetsuisse Faculty ZH, University of Zurich, Switzerland
[10]Stem Cell Research Unit, Medical University of Graz, Austria.

*These authors contributed equally to this work

 # Addresses for correspondence:

Christian Templin, MD
University Hospital Zurich, Department of Cardiology
Rämistr. 100, 8091 Zürich, Switzerland
Phone: +41 44 255 9585; Fax: +41 44 255 4401
E-mail: Christian.Templin@usz.ch

Ulrich Martin, PhD
Leibniz Research Laboratories for Biotechnology and Artifical Organs, Cardiothoracic, Transplantation and Vascular Surgery, Hannover Medical School,
Carl-Neuberg-Str. 1, 30625 Hannover, Germany
Phone: +49 511 532 8820; Fax: +49 511 532 8819
E-mail: martin.ulrich@mh-hannover.de

Total word count: 7000

Abstract

Background: Evaluation of novel cellular therapies in preclinical large animal models and patients is currently hampered by the lack of suitable imaging approaches that allow for long term monitoring of viable transplanted cells. The present study was designed to evaluate sodium iodide symporter (NIS) transgene imaging as a novel approach to follow long term *in vivo* survival, engraftment and distribution of human induced pluripotent stem cell (hiPSC) derivatives in a pig model of myocardial infarction.

Methods and Results: Transgenic hiPSC lines stably expressing a fluorescent reporter and NIS (NIS^{pos}-hiPSCs) were established. Iodide uptake, efflux and cell viability of NIS^{pos}-hiPSCs was assessed *in vitro*. 10 ± 2 days after induction of myocardial infarction by transient occlusion of the left anterior descending artery, catheter-based intramyocardial injection of NIS^{pos}-hiPSCs guided through 3D NOGA™ mapping was performed. Longitudinal dual isotope SPECT-CT imaging was applied using ^{123}I to follow donor cell survival and distribution, and ^{99m}TC-tetrofosmin for myocardial perfusion imaging.

In vitro, iodide uptake in NIS^{pos}-hiPSCs was increased 100-fold above non-transgenic controls. *In vivo*, viable NIS^{pos}-hiPSCs could be visualized at the injection sites for up to 15 weeks. This was confirmed through immunohistochemistry demonstrating that hiPSC-derived endothelial cells contributed to intramyocardial vascularisation. Up to 12-15 weeks after transplantation, no undifferentiated hiPSCs or teratoma were detected.

Conclusions: The present study describes for the first time the feasibility of repeated long term *in vivo* imaging of viability and tissue distribution of cellular grafts in the heart and other organs of large animals. Moreover, this is the first report demonstrating vascular differentiation and long term engraftment of hiPSCs in a large animal model of myocardial infarction. NIS^{pos}-hiPSCs represent a valuable tool to monitor and improve current cellular treatment strategies in clinically relevant large animal models.

Key words:

Imaging, sodium iodide symporter (NIS), induced pluripotent stem cells, iPS cell, myocardial infarction, pig

Introduction

Stem cell-based therapies are being actively explored as a potentially innovative therapeutic strategy for various genetic and acquired diseases. Recently, the possibility to reprogram human somatic cells into induced pluripotent stem cells (hiPSCs) that are able to differentiate into all cell lineages present in the heart[1-4] has opened novel opportunities for myocardial repair. With respect to the potential therapeutic application of pluripotent stem cell derivatives, major progress has been achieved concerning scalable cell production[5, 6] and more efficient and specific differentiation into cell types of interest.[7]

However, there are still major hurdles and risks to overcome with regard to pluripotent stem cell-based heart repair. These include safety risks, especially the potential of teratoma and tumor formation,[2] low cell retention and engraftment rates,[8-11] and the general question of whether engraftment of hiPSC after simple intramyocardial cell injection leads to formation of functional tissue, such as *de novo* vasculature or myocardium, and results in significant clinical benefits.[12] Although some of these issues can be addressed *in vitro* or in appropriate small animal models, others will require exploration in large animal models, which are more similar to humans.[13] Transplanted human cardiomyocytes, for example, are unlikely to fully functionally integrate with rodent myocardium due to highly dissimilar beating rates.[11] Therefore, meaningful assessment of human cells for heart repair has to be demonstrated in large animal models such as dogs, pigs or monkeys.[13]

Clearly, advanced imaging technologies allowing for longitudinal tracking of cellular grafts ideally enabling monitoring of donor cell survival, proliferation, distribution or even differentiation are crucial for (pre-)clinical evaluation of novel cell-based therapeutics.[14] At present, transgene based imaging approaches that fulfill these requirements are mainly restricted to far-red fluorescence reporters or photon-emitting technologies, in particular based on luciferase expression. Unfortunately limited tissue penetration restricts application of these technologies to small animal models, only.[15]

Most or previous large animal studies applied magnetic resonance imaging (MRI) technology to detect nanoparticle-labelled cells.[16] Main disadvantage of this approach is the inability to discriminate vital donor cells from nanoparticle-loaded cell debris or recipient's cells such as macrophages, which can actively incorporate cell debris and released nanoparticles by phagocytosis.[16] In other studies direct radionuclide labeling of cells was performed e.g. through fluorine 18-fluorodeoxyglucose (^{18}F-FDG), Indium-111 (In^{111})-oxine, ^{64}Cu-PTSM or technetium-99 (^{99m}Tc)-Hexamethylprophylene amine oxine.[16] Limitations of the latter techniques include isotope half-time- and label-retention-dependent loss of signal strength.[16] In addition, direct labeling strategies with nanoparticles or radionuclides, particularly for In^{111}, have been reported to affect (stem-) cell vitality.[16]

In a first pilot study to overcome these critical drawbacks, herpes simplex thymidine kinase (HSVtk)-mediated phosphorylation of [^{18}F] FHBG was evaluated as a transgene-based imaging approach in large animals,[17, 18] but detection of transplanted cells was reported several hours after cell injection, only.

Another promising approach has recently been developed,[19] which permits detection of viable transplanted cells by positron emission tomography (PET) or single photon emission computed tomography (SPECT) after iodide (^{123}I) or ^{99m}Tc radiotracer administration. This technology relies on the expression of a transgenic sodium-iodide-symporter (NIS)[20] in transplanted donor cells. Physiological expression of NIS in the adult organism is restricted to the thyroid, stomach, choroids plexus and salivary gland and is not detectable in limbs, brain or other internal organs such as the heart.[20] NIS-mediated iodide accumulation in the thyroid is an active transport process that occurs at the basolateral plasma membrane of the thyroid follicular cells against the iodide electrochemical gradient stimulated by thyroid-stimulating hormone (TSH), and can be specifically inhibited by perchlorate. Clinically, NIS expression provides the basis for the effective diagnostic of thyroid cancer and its metastases by iodide isotope administration.[20]

The technology provides important advantages with respect to clinical application for longitudinal tracking of stem cell grafts. This includes the lack of immunogenicity of the human NIS transgene and the fact that SPECT scanning of radiotracers such as ^{99m}Tc and ^{123}I is widely available at relatively low costs and approved by the responsible regulatory authorities such as the Food and Drug Administration. Moreover, recent progress in quantification of tracer signals using clinical SPECT systems[21] underlines the potential of this approach for tracking cellular transplants in large animals and patients. To date, however, the strategy was evaluated, only, in a small animal model focused on detection of acute cell retention following administration of heart-derived stem cells.[19]

Here we demonstrate the applicability of this technology for *in vivo* monitoring of cellular grafts in a pig model of myocardial infarction. SPECT-CT imaging results revealed successful *in vivo* donor cell labeling by intracoronary iodide administration 5 days or 12 / 15 weeks after intramyocardial cell transplantation. These data were confirmed by immunohistochemistry on harvested tissue providing unequivocal evidence for long term survival, engraftment and differentiation of transplanted human iPSC derivatives.

Methods

Culture of hiPSCs

Conventional culture of hiPSCs was performed as previously described.[1] Mass cell generation of NIS^{pos}-hiPSCs in suspension cultures was performed as previously described.[5, 6]

Generation of sodium-iodide symporter transgenic hiPSC (NIS^{pos}-hiPSC) lines

See supplements for details.

Characterization of NIS^{pos}-hiPSCs

See **Figure 1** and supplements for details.

Iodide uptake and efflux

See supplements for details.

Ex vivo cardiac SPECT-CT imaging

For assessing the SPECT-CT detection limit in terms of prelabelled NIS^{pos}-hiPSCs, cells were incubated for 90 minutes with 1 MBq ^{123}I per 1 x 10^6 cells. After vigorous washing, serial cell dilutions comprising a total of 1 x 10^4, 1 x 10^5, 5 x 10^5, 1 x 10^6, 3 x 10^6, 6 x 10^6 or 1.2 x 10^7 labelled cells were injected into the lateral and septal wall of the left ventricle. The ^{123}I signal was visualized through a dual-detector hybrid SPECT-CT (Infinia Hawkeye, GE Healthcare). In order to mimic *in vivo* imaging, heart derived ^{123}I signals were recorded through a dissected pig chest that was placed above the heart to mimic signal attenuation.

Large animal model

Female landrace pigs (Large White Duroc, Sidler, Zurich, Switzerland; n = 13; 25 - 30 kg;

aged 8 - 10 weeks) were investigated in the present study. Animals were immunosuppressed with cyclosporine A (Novartis Pharmaceuticals, East Hanover, New Jersey; 10 mg / kg body weight daily) and prednisolone (Pfizer, Zurich, Switzerland; 2.5 mg / kg body weight daily) starting 5 days before hiPSC transplantation until animals were sacrificed. Furthermore, all animals received 2 x 400 mg / d dronedarone at the first pre-operative and operative day, and 2 x 200 mg / d from the first post-operative day until the end of the study. All procedures were approved by the responsible local authorities and performed according to the *Guide to the Care and Use of Experimental Animals* published by the U.S. National Institutes of Health (NIH Publication 85-23, reviewed 1996). A detailed description of the study design is shown in **Figure 2**.

Induction of myocardial infarction

Myocardial infarction was created by inflating the balloon for 180 min in the mid-segment of the LAD followed by reperfusion. See supplements for details.

Electromechanical mapping

3D NOGA™ mapping (Biologics Delivery Systems, Biosense Webster, Johnson & Johnson, Irvindale CA) was performed 10 ± 2 days after induction of myocardial infarction to assess electrophysiological tissue viability patterns and wall motion abnormalities. The catheter was placed through the right carotid sheet across the aortic valve into the left ventricle. By navigating the catheter along the endocardium, the local intracardiac electrogram together with the wall motion was recorded from its tip at multiple endocardial sites, and detailed three-dimensional electromechanical maps of the left ventricle were generated. The unipolar voltage values were colour-coded (visualizing infarct zones as red and viable tissue as green to purple) and superimposed on the three-dimensional geometry of the map. NOGA™ mapping and injections were performed as previously described.[22]

Intramyocardial cell injections

1 x 10^8 hiPSCs were labelled with 100 Mbq of ^{123}I (1 Mbq = 1 x 10^6 cells) for 90 min prior to cell injection. Subsequently, cells were washed twice in PBS and were resuspended in PBS as delivery medium, which was supplemented with fluorospheres (Molecular Probes) to enable unequivocal identification of the cell injection sites under UV light during tissue sampling in sacrificed animals (See **Supplemental Figure 1**). Cell injection was performed with a 8F MyoStar injection catheter (Biosense-Webster) using a 27-G needle as follows: three sites with each eight single 250 µl injections were selected (left ventricle anterior wall: 50 million control cells (human mesenchymal stem cells, hMSCs), lateral and septal wall: 50 million NIS^{pos}-hiPSCs, or 50 million NIS^{pos}-hiPSCs mixed with 50 million hMSCs). Control animals received PBS injections at corresponding injection sites. Exact positions of individual injection sites were documented by NOGA™ mapping.

Computed tomography angiography

For cardiac computed tomography angiography 1 ml / kg body weight iodixanol (Visipaque 320 mg / ml, GE Healthcare, Bucks, UK) at a flow rate of 4 - 5 ml / s followed by 50 ml saline solution was injected into the ear vein via a 20-gauge catheter. All scans were performed using the 64-detector CT-component (LightSpeed VCT, GE Healthcare) of a SPECT-CT scanner with prospective ECG-triggering, as previously established and described in detail.[23] Images were analysed on an external workstation (AW 4; GE Healthcare).

Full body CT scanning was performed on the same CT scanner using 100 ml iodixanol.

SPECT imaging

For assessment of myocardial perfusion, ^{99m}TC (10 MBq / kg) was injected into the ear vein and images were acquired over 5 minutes on the SPECT part of a hybrid SPECT-CT scanner (Discovery NM CT 570c, GE Healthcare) integrating a 64-slice CT-device and a

cadmium-zinc-telluride (CZT) gamma camera. The CZT camera has been extensively described recently.[24, 25] Briefly, it is a gamma detector with a pinhole collimator and 19 stationary detector modules positioned around the chest. For perfusion imaging a symmetric energy window of at 140 kiloelectron volt (keV) ± 5 % was used, while for dual peak acquisition with ^{123}I a window at 159 keV ± 5 % was added.

For mid (5 days after transplantation) and long term (12 - 15 weeks after transplantation) detection of transplanted hiPSCs, ^{123}I was injected intracoronary into each main coronary artery (LAD, LCX, RCA) using an over the wire balloon catheter during three coronary occlusions, each lasting 2-3 min. Between occlusions, the coronary artery was reperfused for 2 min. Afterwards, animals underwent SPECT-CT imaging as described above.

See also **Supplemental Figure 2** for details.

(Immuno-)histological analysis

See details in supplements.

Results

Functional sodium iodide symporter expression in transgenic hiPSC clones

hiPSCs (clone hCBiPSC2)[1] were co-transfected with the bicistronic vector pCAG_rNIS_IRES2_Venus_nucmem (**Figure 1A**) and the plasmid αMHCneoPGKhygro[26], enabling selection of hygromycin resistant transgenic cell clones. 6 independent Venus^{pos} clones (designated rNIS clone 1, 2, 4, 5, 6, 7) were analysed for stability of transgene expression. Flow cytometry and fluorescence microscopy revealed robust and stable Venus expression for up to 23 passages with line-specific variations (**Figure 1B&C**). Venus-specific immunohistological assessment was also performed on paraffin sections of suspension culture-derived cell aggregates and differentiated cells in embryoid bodies. In contrast to the expected Venus fluorescence signal in the nucleus of viable cells (**Figure 1C**), cytoplasmic staining was noted post fixation and immunohistochemistry (**Figure 1D** left panel), however, staining specificity was proven by isotype- (**Figure 1D** right panel) and non-transgenic cell controls (data not shown). Quantitative RT-PCR revealed co-expression of the NIS-transgene in Venus expressing clones (data not shown). Venus protein expression was demonstrated in undifferentiated as well as differentiated cells of the NIS^{pos}-hiPSC clone 6 including hiPSC-derived CD31^{pos} endothelial cells (**Supplemental Figure 3**). Further analyses and all cell transplantation experiments were conducted using the NIS^{pos}-hiPSC clone 6.

Transgenic cells and control hiPSCs were analysed for NIS-specific iodide uptake by *in vitro* incubation with ^{125}I, an isotope with a half-life of 13 hours. Intracellular labeling efficiency depends on the effective half-life of an applied isotope and the cells' kinetics of respective isotope accumulation. ^{125}I uptake in NIS^{pos}-hiPSCs reached a plateau after ~ 90 min. After vigorous washing ^{125}I accumulation was ~ 100 times higher than for non-transgenic hiPSC control cells (**Figure 1E**). Importantly, iodide uptake was completely blocked by the specific NIS-inhibitor perchlorate. Typically, the majority of accumulated ^{125}I was released to the medium within 2 h (**Figure 1F**). Notably, neither NIS expression

nor radiolabeling of NIS^{pos}-hiPSCs did affect the cell viability (**Supplemental Figure 4**).

Successful SPECT-CT-based detection of down to 1x10^5 ^{123}I-labelled NIS^{pos}-hiPSCs in explanted pig hearts

Ex vivo cardiac SPECT-CT was performed to determine the detection limit for ^{123}I–pre-labelled NIS^{pos}-hiPSCs after intramyocardial cell injection. Equal volumes of a serial dilution of labelled cells were applied. As shown in **Figure 3**, SPECT-CT enabled detection of a minimum of 1 x 10^5 cells injected into explanted pig hearts. Notably, ^{123}I tracer uptake was detected through a dissected pig chest that had been placed above the heart to mimic signal attenuation *in vivo*. Based on these results 5 x 10^7 pre-labelled NIS^{pos}-hiPSC were subsequently applied *in vivo* per injection areal with a hypothetic detection threshold of ~ 2 % persistent cells.

Pre-labelled NIS^{pos}-hiPSCs were detected for up to 5 hours after catheter-based intramyocardial delivery into distinct regions of infracted hearts

As indicated in the study design (**Figure 2**), myocardial infarction was induced in 13 animals, 10 of which were enrolled in the study. Ten days after transient occlusion of the LAD, SPECT-CT imaging revealed perfusion defects in the apex and mid-segment of the anterior and septal wall in all treated animals (**Figure 4**, 1st line). This was also confirmed by NOGA™ mapping demonstrating loss of electrical activity at the apicoseptal, apicobasal and apicolateral myocardial regions (red colour). Brown points represent the locations of the NOGA™-guided intramyocardial injections at the border zone of infarction (**Figure 4**, 2nd line; **Supplemental Figure 5**). One to three hours after injection of ^{123}I pre-labelled NIS^{pos}-hiPSCs (5 x 10^7 hiPSCs, or 5 x 10^7 hiPSCs co-administered with 5 x 10^7 human MSCs, respectively, per injection area), intensive ^{123}I signals were detected by SPECT-CT imaging in the septal and lateral wall of the left ventricle corresponding exactly to the injection site as recorded by NOGA™-mapping. As expected, ^{123}I treated control cells injected into a separate region of the same heart did not result in a

detectable SPECT signal (**Figure 4**, 3rd line). Notably, MSC co-administration considerably increased signal intensity suggesting improved hiPSC retention in the myocardium after transplantation (**Figure 4 and Supplemental Online Video 1**). The signal intensity was highest in the first hour after cell transplantation and diminished successively. At 3 - 5 hours post injection signal intensity was substantially reduced (**Supplemental Figure 6**) and became undetectable after 24 h (data not shown). Imaging of control animals treated with PBS did not show any SPECT signal (data not shown). As expected, immunohistological staining of tissue sections of the region where NIS^{pos}-hiPSCs and human MSCs had been co-injected, showed an injection channel filled with rounded cells containing a fraction of $Venus^{pos}$ and $OCT4^{pos}$ cells (**Figure 4**). A semiquantitative analysis of the obtained ^{123}I signals in the two pigs that have been sacrificed after day 1 follow up demonstrated that the NIS^{pos}-hiPSCs co-transplanted with MSCs gave a 6.8-fold / 1.7-fold stronger ^{123}I signal than the separately transplanted NIS^{pos}-hiPSC cells (**Supplemental Figure 7**). No detectable ^{123}I activity was associated with the transplanted NIS^{neg} control cells. These results are now presented in **Supplemental Table 1** of the revised manuscript.

Long term detection of engrafted NIS^{pos}-hiPSC derivatives for up to 15 weeks by SPECT-CT imaging following intracoronary iodide administration

For detection of transplanted NIS^{pos}-hiPSC derivatives at 5 days and 12 - 15 weeks post intramyocardial cell injection, ^{123}I was infused intracoronary via LAD, LCX and RCA. One hour after tracer injection, the resulting ^{123}I signals were assessed. As expected, in SPECT-CT a very strong uptake was observed in the thyroid while a weaker uptake was detected in the stomach (data not shown). Interestingly, in the heart, ^{123}I signals were detected exclusively in regions where NIS^{pos}-hiPSCs had been co-transplanted with human MSCs (**Figure 5**). In independent hearts, ^{123}I accumulation was either detected in the lateral heart region or in the septal left ventricular wall, respectively, always correlating with the area of NIS^{pos}-hiPSC / MSC co-injection. In contrast, no ^{123}I signal

could be detected in regions where NIS^{pos}-hiPSCs only or control cells had been injected. *In vitro* co-culture experiments under hypoxic conditions were performed, in order to investigate whether anti-apoptotic effects of MSCs might support the survival of NIS-hiPSCs. Interestingly, MSCs significantly decreased the rate of NIS-hiPSCs apoptosis. This effect was dependent of both secreted factors and cell-cell contact (**Supplemental Figure 8**).

After SPECT-CT, hearts were sacrificed for tissue sample analysis. In correlation with SPECT-CT imaging and NOGA-mapping of myocardial infarction, histological analyses of respective heart regions (collected 5 days and 15 weeks after cell transplantation) revealed typical signs of infarction and subsequent fibrosis including widespread replacement of myocardium through loose to densely arranged cells with fibroblast phenotype, and moderate presence of granulocytes and lymphocytes. Immunohistochemistry confirmed persistent engraftment of NIS^{pos}-hiPSCs. Anti-Venus-specific staining demonstrated the presence of Venus^{pos} hiPSC derivatives 5 days and 12 / 15 weeks after cell injection. Notably, after 12 / 15 weeks the histological images suggest that hiPSC derivatives had adopted an endothelial phenotype lining numerous vessels in the injected heart regions (see **Figure 5** right panel, **Supplemental Figure 9**). Complementing semi-quantitative analyses on the capillary densities of the respective heart regions suggested an increased capillary density in the regions of NIS^{pos}-hiPSC-MSC versus NIS^{pos}-hiPSC injection (**Supplemental Figure 10**). Interestingly, in contrast to analysis 5 hours post cell administration, no OCT4-specific cell staining could be detected at 5 days or 12 / 15 weeks (data not shown). Also, no teratoma or other obvious tumor formation was detected in the sacrificed recipient animals during autopsy.

Discussion

The availability of transgene-based imaging technologies in large animals that enable non-toxic, specific, sensitive, non-invasive and serial long term imaging of viable grafts is

of utmost importance for pre-clinical evaluation of stem cell based therapies.

We have here established a reporter gene approach that enables *in vivo* monitoring of long term survival of human iPSC derivatives in a pig model of myocardial infarction. Notably, this is the first report demonstrating the feasibility of repeated longitudinal *in vivo* imaging of cell viability, proliferation and tissue distribution of cellular grafts in internal organs of large animals.

Similar to luciferase imaging in small animals, viable cells expressing NIS are able to accumulate ^{123}I and to evoke a detectable SPECT signal, thereby preventing false positive detection of dead cells, cell debris-bound label or phagocytosing macrophages. Although the ratio of the intensity of the specific ^{123}I signal in our NIS^{pos}-hiPSCs compared to NIS^{neg} hiPSCs as determined *in vitro* is lower than the typical signal to background ratio in case of luciferase reporter systems, long term surviving NIS^{pos}-hiPSCs derivatives evoked a ^{123}I signal of considerable intensity in the areas of intramyocardial cell injection. This may be explained by the relatively low absorption of the ^{123}I signal through soft and hard tissue and is in contrast to the very limited tissue penetration of luciferin emitted light, which, even in small animals with low tissue thickness, leads to significant loss of signal.

Ex vivo injection of ^{123}I-labelled NIS^{pos}-hiPSCs revealed a detection limit of ~ 1 x 10^5 cells in isolated pig hearts. Since ^{123}I signals were recorded through an isolated pig chest, one can expect signal intensities *in vivo* in the same range as those detected in hearts assessed *ex vivo*. Although not directly comparable, because i) lentiviral vectors and another tracing approach were used, ii) another stem cell type, namely cardiac stem cells, was applied, and iii) signal retention through pig chest is slightly different from retention by a rat chest, the determined detection limit is in the same range than for cell transplantation into rat hearts. Here, Terrovitis et al.[19] estimated 1.5 x 10^5 as minimal detectable cell number. Further advantages of hNIS-SPECT versus HSVtk-PET imaging are the wide availability of the necessary tracers and lack of need for specialized radiosynthesis facilities, and the lack of immunogenicity of the human NIS, which may be

of critical importance especially for long term monitoring.

Obviously, SPECT imaging of NIS-expressing cell grafts has limitations. As every *in vivo* imaging approach, there is a detection limit in terms of a minimal detectable number of cells. Certainly, we cannot exclude distribution of single undifferentiated or differentiated hiPSC derivatives to other organs. Indeed, only if a critical number of cells accumulate or is reached due to local proliferation, the minimal detection limit at a specific site is achieved, NIS-expressing engrafted cells can be detected. Nevertheless, in our experiments, we were not able detect any ^{123}I signals outside the heart despite the naturally NIS expressing tissue sites. Autopsies of the sacrificed animals 12 - 15 weeks after cell infusion confirmed these results and did not reveal any sign of tumour or teratoma formation. Together with the absence of OCT4^{pos} cells 12 - 15 weeks after cell transplantation as analysed by immunohistochemistry, this raises the question whether the high incidence of teratomas observed in immunoincompetent mice are actually indicative for clinical applications, or rather an artefact of species incompatibilities that prevent natural control of cell proliferation in the specific tissue niches. Another potential explanation for the obvious absence of undifferentiated cells and the observed parallel persistence of differentiated vascular NIS^{pos}-hiPSC derivatives might be the applied immunosuppressive protocol consisting of relative high doses of cyclosporine A (CsA) and prednisolone. In general, the long term persistence of hiPSC-derived endothelial cells indicates the efficacy of our immunosuppressive protocol, at least in terms of T-cell reactivity towards differentiated iPSC derivatives. However, there is evidence that CsA is not effective towards natural killer (NK) cells,[27] which might lead to selective NK cell-based erasure of undifferentiated pluripotent stem cells.[28] In case of prednisolone, recent data suggest that inhibition of NK cells depends on the mode of activation thereby indicating that prednisolone treatment might also not fully prevent NK-mediated killing of undifferentiated hiPSCs.[29]

Another limitation of this imaging technology is the physiological expression of NIS in the thyroid, stomach, choroids plexus, and salivary gland. As the signals from these

organs are strong, they may cover up weak signals from adjacent organs. For instance, although not posing a problem in larger animals such as the pig, the strong thyroid signal may interfere with close-by cardiac tracer signals in mice. Also, the stomach background signal may interfere with tracer signals in the upper abdomen.

Of course, there is room for further improvements: Higher levels of NIS^{pos} expression in optimized vector systems and selected stable cell clones might lead to further increase of ^{123}I accumulation compared to NIS^{neg} control cells. In addition, we do currently not know, whether potential silencing effects during *in vivo* differentiation of the transplanted NIS^{pos}-hiPSCs might have diminished NIS expression in our experiments, and whether expression systems with reduced silencing can lead to further increase of the ^{123}I signal.

As mentioned above, immunohistochemical staining of myocardial tissue sections harvested 5 days and 12 - 15 weeks after cell application showed no $OCT4^{pos}$ cells in the areas of previous cell infusion. Instead, $Venus^{pos}$ NIS^{pos}-hiPSC derivatives with endothelial phenotype were detected, which contributed to the intramyocardial vasculature. Notably, the utilized CAG promoter driven NIS does not allow following differentiation events through SPECT imaging. However, this could be realized through placing NIS under control of cell-type specific promoters, for instance the OCT4 promoter[5] or the cardiomyocyte specific αMHC promoter.[30]

Of importance for future clinical application of this technology will be the use of well characterised transgenic cell clones with defined transgene integration through zinc finger or TALE nuclease,[31] for instance, in safe harbour sites such as adeno-associated virus integration site 1 (AAVS1),[31] thereby diminishing risks of insertional mutagenesis and carcinogenesis. Importantly, it has to be assessed whether the required level of radiation can be reduced: Although the applied ^{123}I dose is on a similar level than clinically applied for standard tumor therapies, it is far higher than for routine thyroid diagnostics thereby prohibiting clinical application of the developed approach at this stage. Furthermore, and

although the conducted minimal invasive cell application by intramyocardially hiPSC injection is of high clinical relevance, it has to be evaluated whether similar or even higher sensitivities and signal-to-noise ratios can be obtained in case of global tracer delivery for instance through the pig's ear veins.

As a first application of the established technology for SPECT imaging of transgenic NIS expression, we have addressed the common problem of low cell survival and retention rates after cell transplantation.[8-10] Typically, after intramyocardial cell infusion the majority of donor cells are directly flushed back through the injection channel[10, 32] or do not survive the initial phase after transplantation.[9] To address this problem, Laflamme et al. recently described a novel pro-survival cocktail that can dramatically increases engraftment of transplanted human embryonic stem cell derived cardiomyocytes in a athymic rat model.[8] We have now investigated whether co-transplantation of human MSCs that release antiapoptotic factors[33] and express immunomodulatory properties[34] may improve the survival and engraftment of transplanted NIS^{pos}-hiPSCs after xenotransplantation into pigs. Interestingly, SPECT imaging suggested a positive effect of the co-transplanted human MSCs even 3 hours after cell infusion showing a markedly stronger tracer uptake at the sites where NIS^{pos}-hiPSCs had been co-transplanted with human MSCs, than at the injection sites of pure NIS^{pos}-hiPSCs. It is questionable, whether this very early phenomenon can be explained through anti-apoptotic effects. It is more likely that other effects including MSC-mediated increased cell aggregation, which may favour engraftment and diminish the flush out of transplanted cells, are responsible for this effect. However, in the mid and long term (5 days and 12 - 15 weeks), NIS^{pos}-hiPSCs could be detected exclusively at the site of co-injection, indicating an additional profound effect on long term engraftment of NIS^{pos} hiPSCs. Certainly, deciphering the underlying mechanisms will require extensive additional investigations but will be of utmost importance to optimize MSC-supported survival of hiPSC derivatives.

Conclusions

This is the first study demonstrating the usefulness of the sodium iodide symporter (NIS) for serial long term tracking of survival, engraftment and distribution of cellular grafts in a large animal model using SPECT-CT imaging. Moreover, for the first time we demonstrate long term survival and differentiation of human iPSCs in a preclinical pig model of myocardial infarction. The applied three dimensional (3D) hybrid imaging protocol enables combined assessment of cardiac anatomy, myocardial perfusion and monitoring of donor cell survival, proliferation and distribution within one imaging modality

Acknowledgments

We are grateful to Birgit Feilhauer, Kristina Mayer and Julia Osipova and for technical assistance with cell production and labeling; Christine DePasquale and Eliane Fischer for help with in vitro studies; Paula Grest for assistance in cutting the organs and Kati Zlinszky for assistance in immunohistochemistry; Michele Sidler for excellent animal anesthesia and Hanspeter Fischer for assistance in NOGA™ mapping.

Funding Sources

The study was supported in part by a grant of the Swiss National Research Foundation 'Sonderprogramm Universitäre Medizin' (Nr. 33CM30-124112/1) and by research grants of the Swiss Life Foundation and the Gottfried and Julia Bangerter-Rhvner-Foundation as well as by the Cluster of Excellence "REBIRTH", the German Ministry for Education and Science (01GN0958), the CORTISS foundation, the Austrian Research Foundation (FFG, grant N211-NAN) and the Adult Stem Cell Research Foundation (TASCRF).

Figure legends

Figure 1: Generation and functional characterization of NIS^{pos}-hiPSCs

(A) Map of the bicistronic vector pCAG_rNIS_IRES2_Venus_nucmem used for the generation of transgenic hiPSC clones.

(B) FACS analysis of Venus expression in several independent rNIS^{pos}-hiPSC clones. Individual clones showed a stable level of transgene expression for up to 23 passages.

(C) Overlay of fluorescence and phase contrast image revealing the expected nuclear Venus localization of a typical NIS^{pos}-hiPSC colony cultured on matrigel (clone 6, 6 passages after clonal selection).

(D) Detection of Venus by immunohistochemistry on a section of PFA-fixed NIS^{pos}-hiPSC aggregates derived from suspension culture, and the respective isotope control. For immunostaining, an anti-GFP antibody was used, which crossreacts with the yellow GFP variant Venus. Notably, fixation and immunohistochemistry treatments leads to an apparently cytoplasmic Venus-specific staining, which is in contrast to the direct Venus fluorescence in viable cells that is strictly restricted to the nuclear membrane as shown in (C).

(E) Kinetics of ^{125}I uptake by NIS^{pos}-hiPSCs (clone 6), inhibition by 100µM perchlorate, and NIS^{neg}-hiPSC controls (mean ± SEM, triplicate measurements). Iodide uptake reached a steady state within 90 min with a max concentration of ~ 100-fold above background in negative controls. ^{125}I accumulation in NIS^{pos}-hiPSCs was completely abolished by perchlorate suggesting specificity of the signal.

(F) Kinetic of iodide retention in NIS^{pos}-hiPSCs (mean ± SEM, triplicate measurements).

Figure 2: Study design

CsA = cyclosporin A, iPSCs = induced pluripotent stem cells; MI = myocardial infarction

Figure 3: *Ex vivo* SPECT-CT of pig hearts transplanted with NIS^{pos}-hiPSCs

^{123}I-prelabeled NIS^{pos}-hiPSCs were transplanted into pig hearts *ex vivo* in order to determine the minimal number of detectable NIS^{pos}-hiPSCs. Depicted are SPECT-CT images of pig hearts after injections of equal volumes with different amounts of cells as indicated: 1 = 1.2 x 10^7; 2 = 6 x 10^6; 3 = 3 x 10^6; 4 = 1 x 10^6; 5 = 5 x 10^5; 6 = 1 x 10^5; 7 = 1 x 10^4. Injected NIS^{pos}-hiPSCs were detectable down to 1 x 10^5 cells.

Figure 4: *In vivo* cardiac hybrid-SPECT-CT demonstrates successful induction of myocardial infarction and suggests long term survival of NIS^{pos}-hiPSC grafts

Representative images of a heart of one of three recipient animals that were sacrificed 6 h after cell injection are shown.

1st line: SPECT-CT *in vivo* imaging of the left ventricle demonstrates a loss of myocardial perfusion (blue) in the anteroapical and septal wall after occlusion of the LAD. Non-infarcted myocardium appears orange coloured indicating normal ^{99m}TC-tetrofosmin uptake.

2nd line: Three-dimensional NOGA™ mapping of the left ventricle recorded during cell injection. NOGA™ colours represent unipolar voltage values, red = scar, green to blue = viable tissue. Cell injection sites in the lateral (NIS^{pos}-hiPSCs + MSCs), septal (NIS^{pos}-hiPSCs) and anterior (non-transgenic MSCs) walls are shown as brown dots.

3rd line: SPECT-CT imaging of left ventricle 1 h after catheter-based intramyocardial cell injection demonstrating intense ^{123}I signals (yellow) in the lateral and septal wall that correspond exactly to the injection sites (each injection area 5 x 10^7 hiPSCs) as recorded by NOGA™ mapping; control cells did not result in a detectable radiotracer signal (anterior wall). Co-administration of MSCs markedly increased signal intensity (lateral wall).

Immunohistochemistry: Depicted are immunohistological sections of the lateral ventricle wall showing a cell injection channel 6 h after cell application filled with co-transplanted hMSCs and Venus^{pos} NIS^{pos}-hiPSCs stained for Venus and OCT4 (each with brown colour)

Figure 5: *In vivo* SPECT-CT imaging of long term surviving derivatives of NIS^{pos}-hiPSCs in pig hearts after 5 days and 15 weeks, respectively

Non-pre-labelled NIS^{pos}-hiPSCs (each site 5x10^7 cells) could be detected in mid-term (5 days) and long term follow up (15 weeks) ~ 1h after intracoronary ^{123}I injection. Immunohistochemical staining of tissue sections of corresponding areas of the left ventricular wall confirmed the presence of Venus^{pos} (stained with crossreacting anti GFP antibody) NIS^{pos}-hiPSC derivatives. Notably, the vast majority of Venus^{pos} iPSC derivatives were found to represent endothelial cells integrated into the cardiac vasculature 15 weeks after cell transplantation. No OCT4^{pos} cells could be detected (data not shown). The ^{123}I-signal intensities as determined by volume of interest analysis (VOI) of the respective animals shown are as follows: 5 days post injection animal: VOI = 4.3 x 10^5 counts (septal region = NIS^{pos}-hiPSC + MSC injection); 15 weeks post injection animal: VOI = 1.8 x 10^5 counts (lateral region = NIS^{pos}-hiPSC + MSC injection).

Disclosures

None.

References

1. Haase A, Olmer R, Schwanke K, Wunderlich S, Merkert S, Hess C, Zweigerdt R, Gruh I, Meyer J, Wagner S, Maier LS, Han DW, Glage S, Miller K, Fischer P, Scholer HR, Martin U. Generation of induced pluripotent stem cells from human cord blood. *Cell Stem Cell*. 2009;5:434-441
2. Mauritz C, Martens A, Rojas SV, Schnick T, Rathert C, Schecker N, Menke S, Glage S, Zweigerdt R, Haverich A, Martin U, Kutschka I. Induced pluripotent stem cell (ipsc)-derived flk-1 progenitor cells engraft, differentiate, and improve heart function in a mouse model of acute myocardial infarction. *European heart journal*. 2011;32:2634-2641
3. Mauritz C, Schwanke K, Reppel M, Neef S, Katsirntaki K, Maier LS, Nguemo F, Menke S, Haustein M, Hescheler J, Hasenfuss G, Martin U. Generation of functional murine cardiac myocytes from induced pluripotent stem cells. *Circulation*. 2008;118:507-517
4. Zhang SJ, Wu JC. Comparison of imaging techniques for tracking cardiac stem cell therapy. *J Nucl Med*. 2007;48:1916-1919
5. Olmer R, Haase A, Merkert S, Cui W, Palecek J, Ran C, Kirschning A, Scheper T, Glage S, Miller K, Curnow EC, Hayes ES, Martin U. Long term expansion of undifferentiated human ips and es cells in suspension culture using a defined medium. *Stem Cell Res*. 2010;5:51-64
6. Zweigerdt R, Olmer R, Singh H, Haverich A, Martin U. Scalable expansion of human pluripotent stem cells in suspension culture. *Nat Protoc*. 2011;6:689-700
7. Murry CE, Keller G. Differentiation of embryonic stem cells to clinically relevant populations: Lessons from embryonic development. *Cell*. 2008;132:661-680
8. Laflamme MA, Chen KY, Naumova AV, Muskheli V, Fugate JA, Dupras SK, Reinecke H, Xu C, Hassanipour M, Police S, O'Sullivan C, Collins L, Chen Y, Minami E, Gill EA, Ueno S, Yuan C, Gold J, Murry CE. Cardiomyocytes derived from human embryonic stem cells in pro-survival factors enhance function of infarcted rat hearts. *Nat Biotechnol*. 2007;25:1015-1024
9. Muller-Ehmsen J, Krausgrill B, Burst V, Schenk K, Neisen UC, Fries JW, Fleischmann BK, Hescheler J, Schwinger RH. Effective engraftment but poor mid-term persistence of mononuclear and mesenchymal bone marrow cells in acute and chronic rat myocardial infarction. *Journal of molecular and cellular cardiology*. 2006;41:876-884
10. Teng CJ, Luo J, Chiu RC, Shum-Tim D. Massive mechanical loss of microspheres with direct intramyocardial injection in the beating heart: Implications for cellular cardiomyoplasty. *J Thorac Cardiovasc Surg*. 2006;132:628-632
11. van Laake LW, Passier R, Doevendans PA, Mummery CL. Human embryonic stem cell-derived cardiomyocytes and cardiac repair in rodents. *Circ Res*. 2008;102:1008-1010
12. Templin C, Luscher TF, Landmesser U. Cell-based cardiovascular repair and regeneration in acute myocardial infarction and chronic ischemic cardiomyopathy-current status and future developments. *The International journal of developmental biology*. 2011;55:407-417
13. Gandolfi F, Vanelli A, Pennarossa G, Rahaman M, Acocella F, Brevini TA. Large animal models for cardiac stem cell therapies. *Theriogenology*. 2011;75:1416-1425
14. Bengel FM, Schachinger V, Dimmeler S. Cell-based therapies and imaging in cardiology. *Eur J Nucl Med Mol Imaging*. 2005;32 Suppl 2:S404-416
15. de Almeida PE, van Rappard JR, Wu JC. In vivo bioluminescence for tracking cell fate and function. *American journal of physiology. Heart and circulatory physiology*. 2011;301:H663-671

16. Ruggiero A, Thorek DL, Guenoun J, Krestin GP, Bernsen MR. Cell tracking in cardiac repair: What to image and how to image. *European radiology*. 2012;22:189-204
17. Lee AS, Xu D, Plews JR, Nguyen PK, Nag D, Lyons JK, Han L, Hu S, Lan F, Liu J, Huang M, Narsinh KH, Long CT, de Almeida PE, Levi B, Kooreman N, Bangs C, Pacharinsak C, Ikeno F, Yeung AC, Gambhir SS, Robbins RC, Longaker MT, Wu JC. Preclinical derivation and imaging of autologously transplanted canine induced pluripotent stem cells. *The Journal of biological chemistry*. 2011;286:32697-32704
18. Willmann JK, Paulmurugan R, Rodriguez-Porcel M, Stein W, Brinton TJ, Connolly AJ, Nielsen CH, Lutz AM, Lyons J, Ikeno F, Suzuki Y, Rosenberg J, Chen IY, Wu JC, Yeung AC, Yock P, Robbins RC, Gambhir SS. Imaging gene expression in human mesenchymal stem cells: From small to large animals. *Radiology*. 2009;252:117-127
19. Terrovitis J, Kwok KF, Lautamaki R, Engles JM, Barth AS, Kizana E, Miake J, Leppo MK, Fox J, Seidel J, Pomper M, Wahl RL, Tsui B, Bengel F, Marban E, Abraham MR. Ectopic expression of the sodium-iodide symporter enables imaging of transplanted cardiac stem cells in vivo by single-photon emission computed tomography or positron emission tomography. *J Am Coll Cardiol*. 2008;52:1652-1660
20. Dohan O, De la Vieja A, Paroder V, Riedel C, Artani M, Reed M, Ginter CS, Carrasco N. The sodium/iodide symporter (nis): Characterization, regulation, and medical significance. *Endocr Rev*. 2003;24:48-77
21. Stodilka RZ, Blackwood KJ, Kong H, Prato FS. A method for quantitative cell tracking using spect for the evaluation of myocardial stem cell therapy. *Nucl Med Commun*. 2006;27:807-813
22. Gyongyosi M, Dib N. Diagnostic and prognostic value of 3d noga mapping in ischemic heart disease. *Nat Rev Cardiol*. 2011;8:393-404
23. Buechel RR, Husmann L, Herzog BA, Pazhenkottil AP, Nkoulou R, Ghadri JR, Treyer V, von Schulthess P, Kaufmann PA. Low-dose computed tomography coronary angiography with prospective electrocardiogram triggering: Feasibility in a large population. *J Am Coll Cardiol*. 2011;57:332-336
24. Buechel RR, Herzog BA, Husmann L, Burger IA, Pazhenkottil AP, Treyer V, Valenta I, von Schulthess P, Nkoulou R, Wyss CA, Kaufmann PA. Ultrafast nuclear myocardial perfusion imaging on a new gamma camera with semiconductor detector technique: First clinical validation. *Eur J Nucl Med Mol Imaging*. 2010;37:773-778
25. Herzog BA, Buechel RR, Husmann L, Pazhenkottil AP, Burger IA, Wolfrum M, Nkoulou RN, Valenta I, Ghadri JR, Treyer V, Kaufmann PA. Validation of ct attenuation correction for high-speed myocardial perfusion imaging using a novel cadmium-zinc-telluride detector technique. *J Nucl Med*. 2010;51:1539-1544
26. Xu XQ, Zweigerdt R, Soo SY, Ngoh ZX, Tham SC, Wang ST, Graichen R, Davidson B, Colman A, Sun W. Highly enriched cardiomyocytes from human embryonic stem cells. *Cytotherapy*. 2008;10:376-389
27. Wai LE, Fujiki M, Takeda S, Martinez OM, Krams SM. Rapamycin, but not cyclosporine or fk506, alters natural killer cell function. *Transplantation*. 2008;85:145-149
28. Drukker M, Benvenisty N. The immunogenicity of human embryonic stem-derived cells. *Trends Biotechnol*. 2004;22:136-141
29. Chiossone L, Vitale C, Cottalasso F, Moretti S, Azzarone B, Moretta L, Mingari MC. Molecular analysis of the methylprednisolone-mediated inhibition of nk-cell function: Evidence for different susceptibility of il-2- versus il-15-activated nk cells. *Blood*. 2007;109:3767-3775

30. Xu XQ, Soo SY, Sun W, Zweigerdt R. Global expression profile of highly enriched cardiomyocytes derived from human embryonic stem cells. *Stem Cells*. 2009;27:2163-2174
31. Hockemeyer D, Wang H, Kiani S, Lai CS, Gao Q, Cassady JP, Cost GJ, Zhang L, Santiago Y, Miller JC, Zeitler B, Cherone JM, Meng X, Hinkley SJ, Rebar EJ, Gregory PD, Urnov FD, Jaenisch R. Genetic engineering of human pluripotent cells using tale nucleases. *Nature biotechnology*. 2011;29:731-734
32. Al Kindi A, Ge Y, Shum-Tim D, Chiu RC. Cellular cardiomyoplasty: Routes of cell delivery and retention. *Front Biosci*. 2008;13:2421-2434
33. Wen Z, Zheng S, Zhou C, Wang J, Wang T. Repair mechanisms of bone marrow mesenchymal stem cells in myocardial infarction. *J Cell Mol Med*. 2011;15:1032-1043
34. Shi M, Liu ZW, Wang FS. Immunomodulatory properties and therapeutic application of mesenchymal stem cells. *Clin Exp Immunol*. 2011;164:1-8

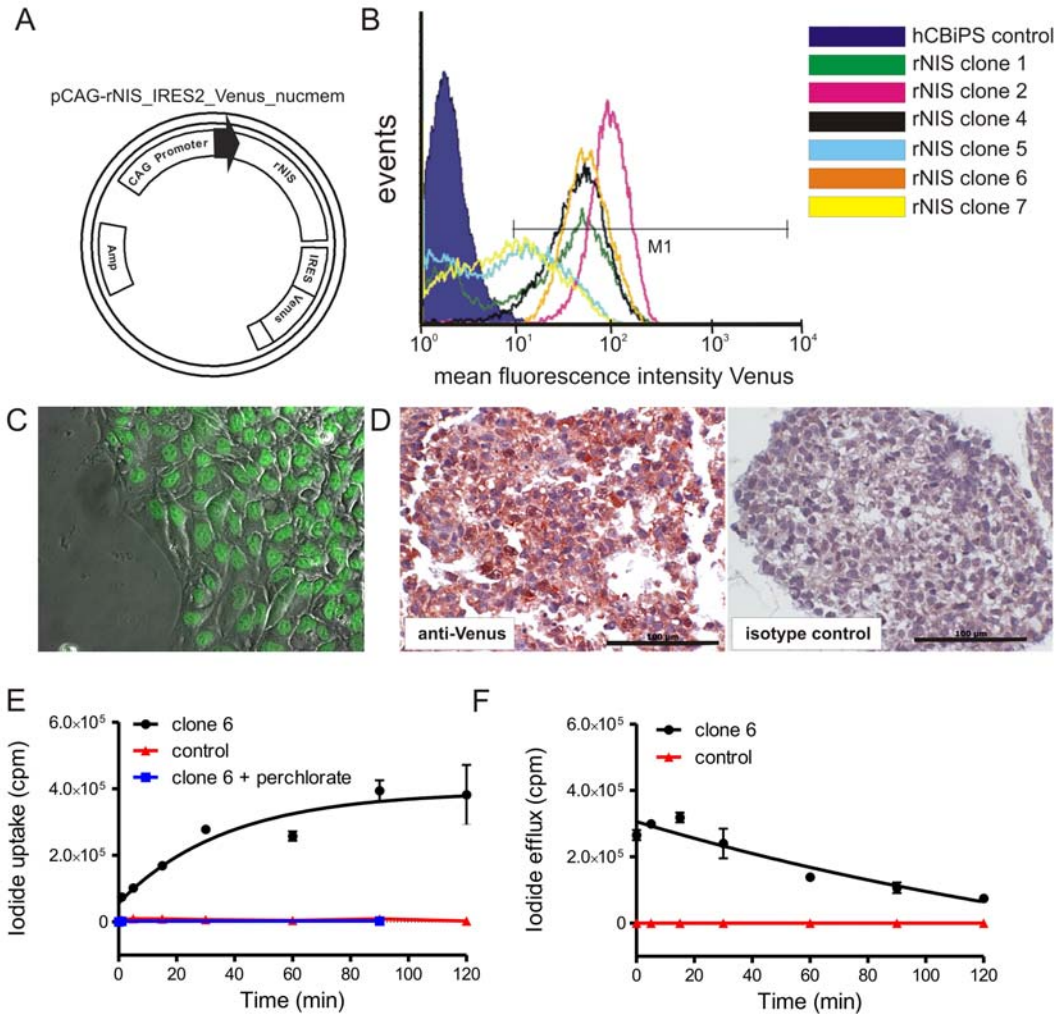
A
pCAG-rNIS_IRES2_Venus_nucmem
CAG Promoter
rNIS
IRES
Venus
Amp
B
events
M1
mean fluorescence intensity Venus
hCBiPS control
rNIS clone 1
rNIS clone 2
rNIS clone 4
rNIS clone 5
rNIS clone 6
rNIS clone 7
C
D
anti-Venus
isotype control
E
Iodide uptake (cpm)
clone 6
control
clone 6 + perchlorate
Time (min)
F
Iodide efflux (cpm)
clone 6
control
Time (min)

Figure 1

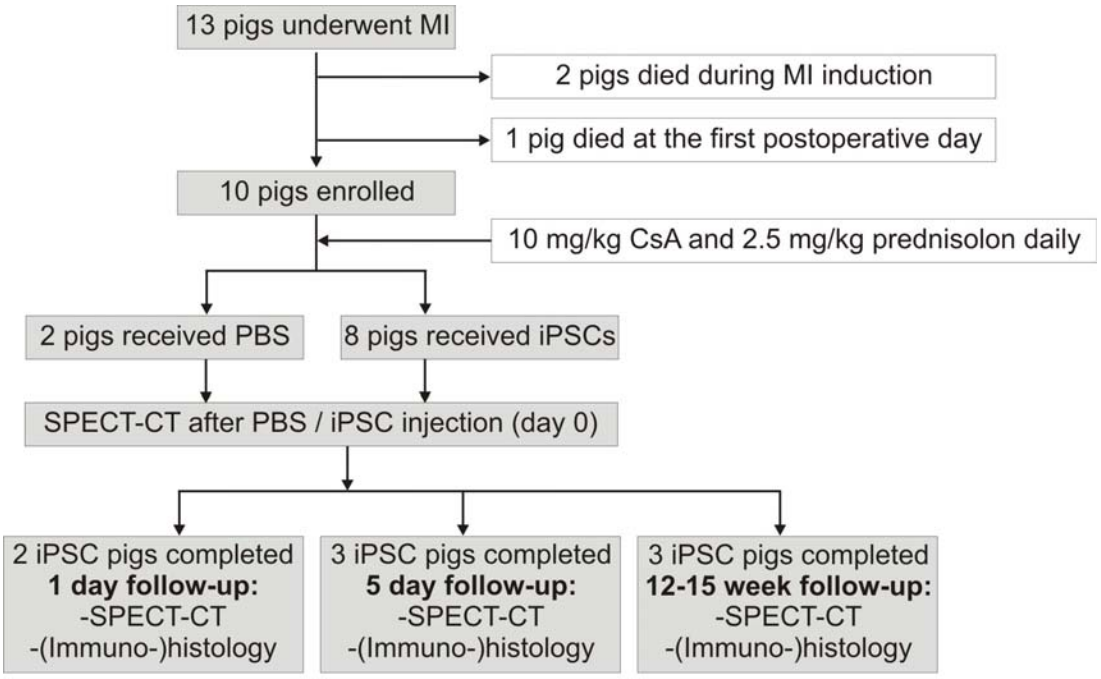

Figure 2

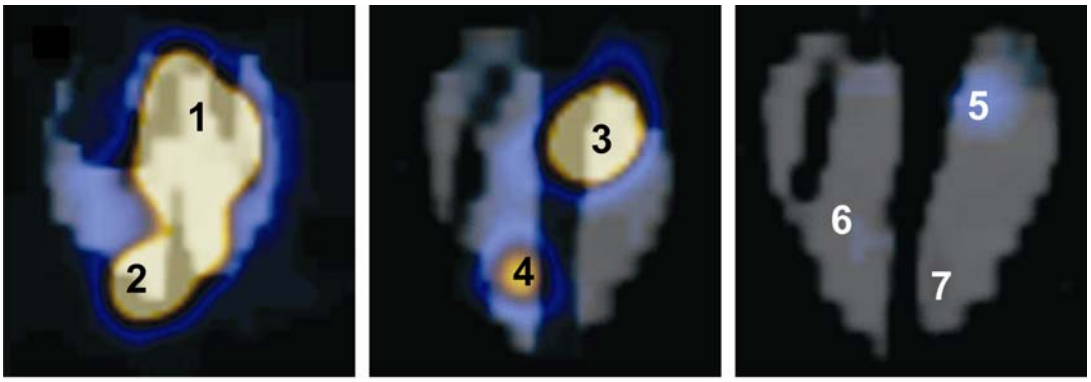

Figure 3

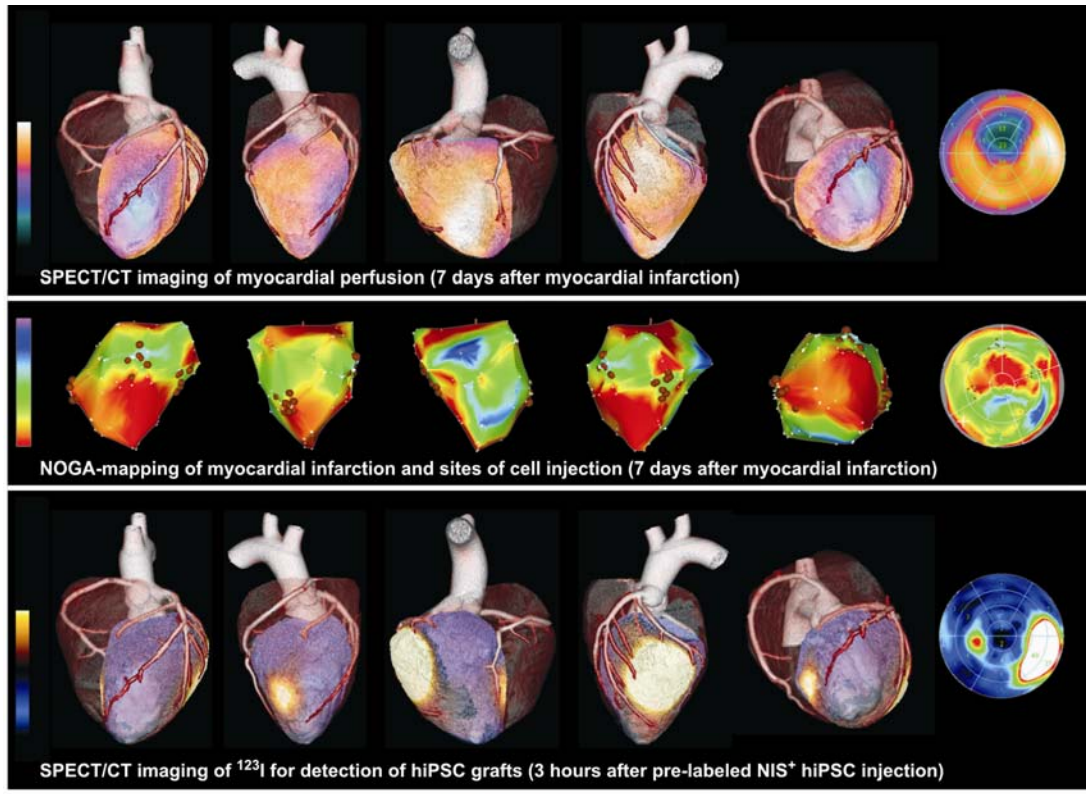
SPECT/CT imaging of myocardial perfusion (7 days after myocardial infarction)
NOGA-mapping of myocardial infarction and sites of cell injection (7 days after myocardial infarction)
SPECT/CT imaging of ^{123}I for detection of hiPSC grafts (3 hours after pre-labeled NIS^{+} hiPSC injection)

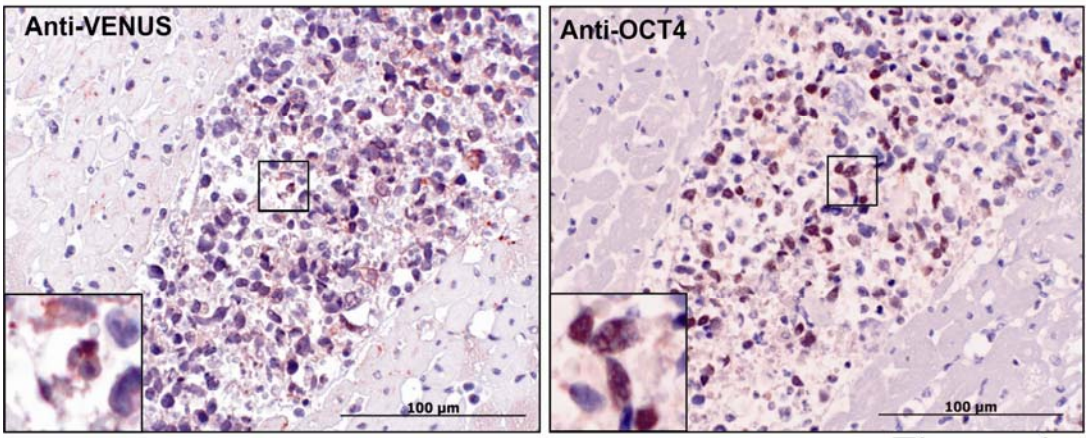
Anti-VENUS
Anti-OCT4
100 µm
100 µm

Figure 4

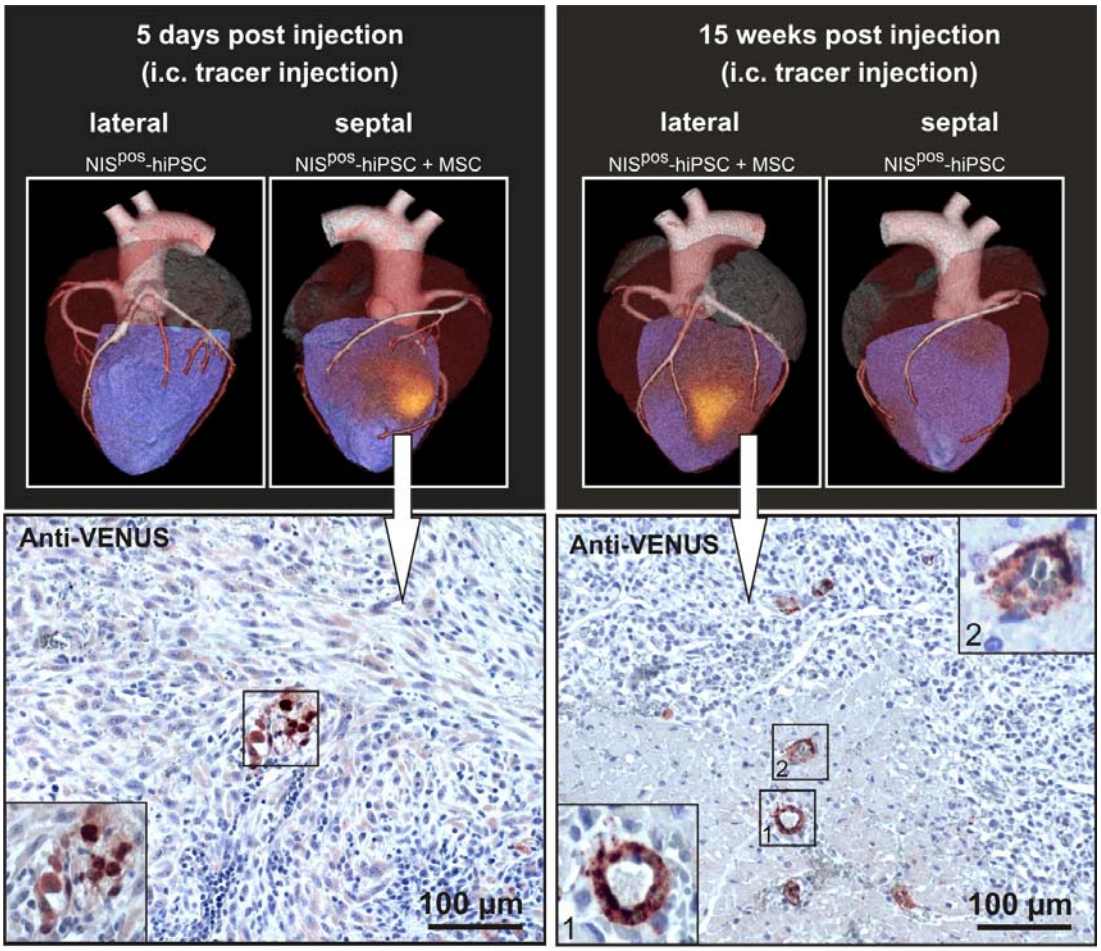
5 days post injection
(i.c. tracer injection)
lateral
septal
NIS^pos-hiPSC
NIS^pos-hiPSC + MSC
15 weeks post injection
(i.c. tracer injection)
lateral
septal
NIS^pos-hiPSC + MSC
NIS^pos-hiPSC
Anti-VENUS
Anti-VENUS
100 µm
100 µm
1
2
2
1

Figure 5

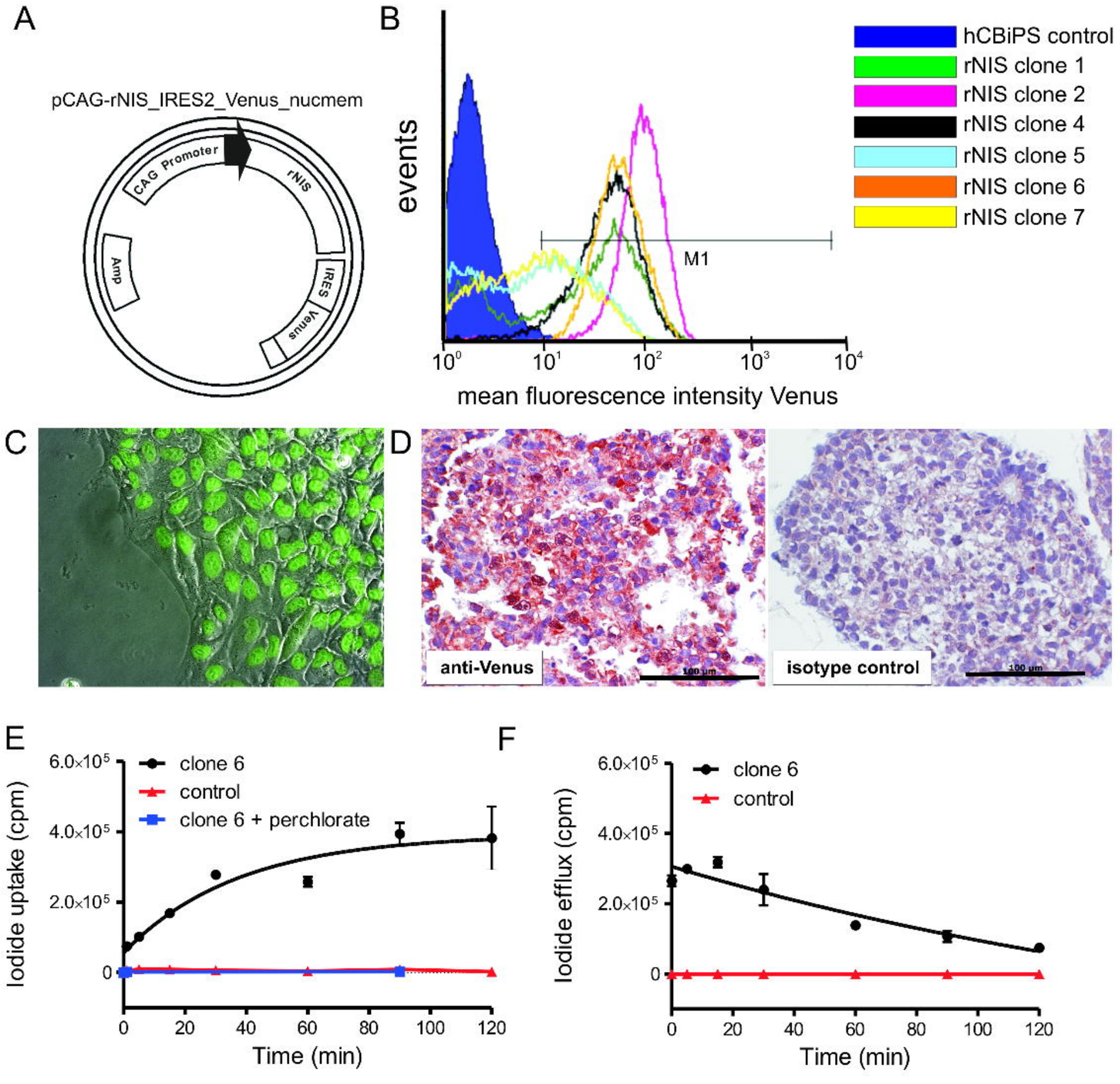
A
pCAG-rNIS_IRES2_Venus_nucmem
CAG Promoter
rNIS
IRES
Venus
Amp
B
events
M1
hCBiPS control
rNIS clone 1
rNIS clone 2
rNIS clone 4
rNIS clone 5
rNIS clone 6
rNIS clone 7
10^0
10^1
10^2
10^3
10^4
mean fluorescence intensity Venus
C
D
anti-Venus
100 µm
isotype control
100 µm
E
Iodide uptake (cpm)
6.0×10^5
4.0×10^5
2.0×10^5
0
clone 6
control
clone 6 + perchlorate
0
20
40
60
80
100
120
Time (min)
F
Iodide efflux (cpm)
6.0×10^5
4.0×10^5
2.0×10^5
0
clone 6
control
0
20
40
60
80
100
120
Time (min)

Figure 1

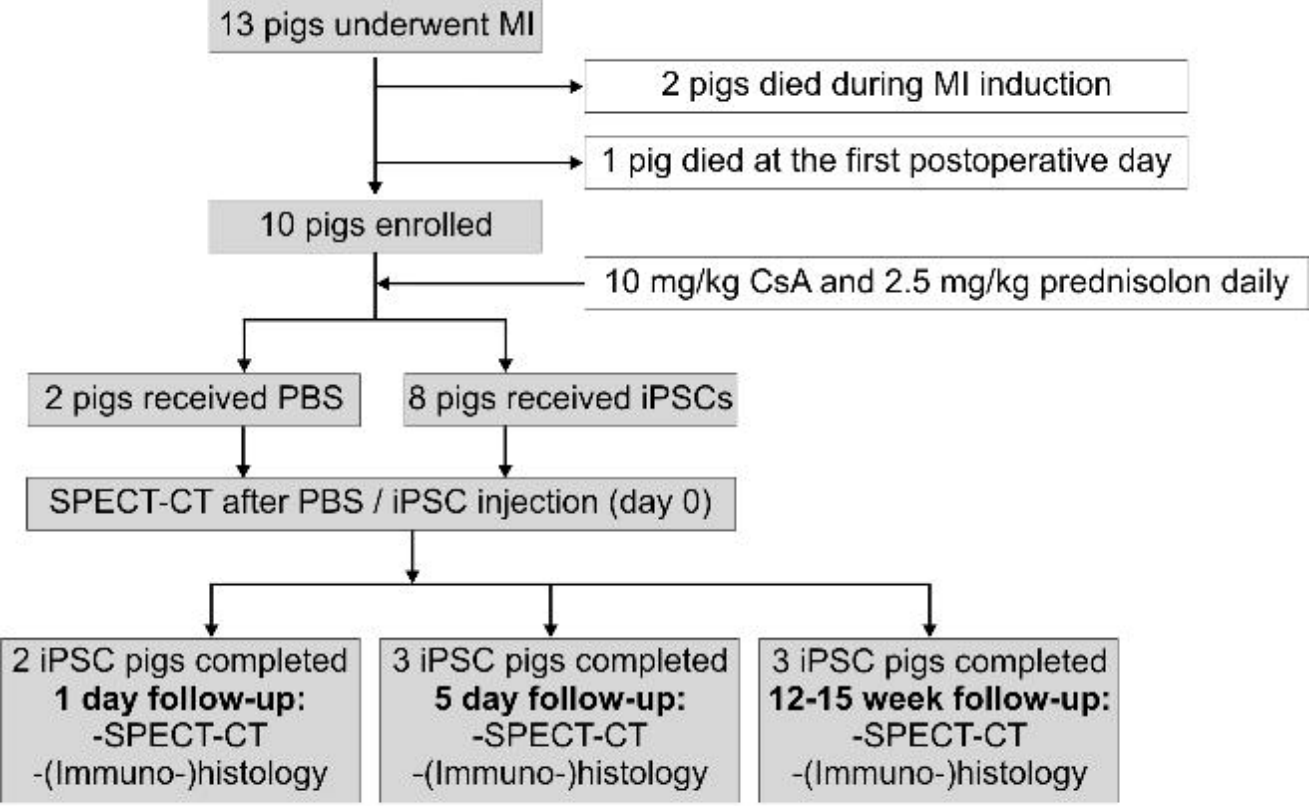
13 pigs underwent MI
2 pigs died during MI induction
1 pig died at the first postoperative day
10 pigs enrolled
10 mg/kg CsA and 2.5 mg/kg prednisolon daily
2 pigs received PBS
8 pigs received iPSCs
SPECT-CT after PBS / iPSC injection (day 0)
2 iPSC pigs completed
1 day follow-up:
-SPECT-CT
-(Immuno-)histology
3 iPSC pigs completed
5 day follow-up:
-SPECT-CT
-(Immuno-)histology
3 iPSC pigs completed
12-15 week follow-up:
-SPECT-CT
-(Immuno-)histology

Figure 2

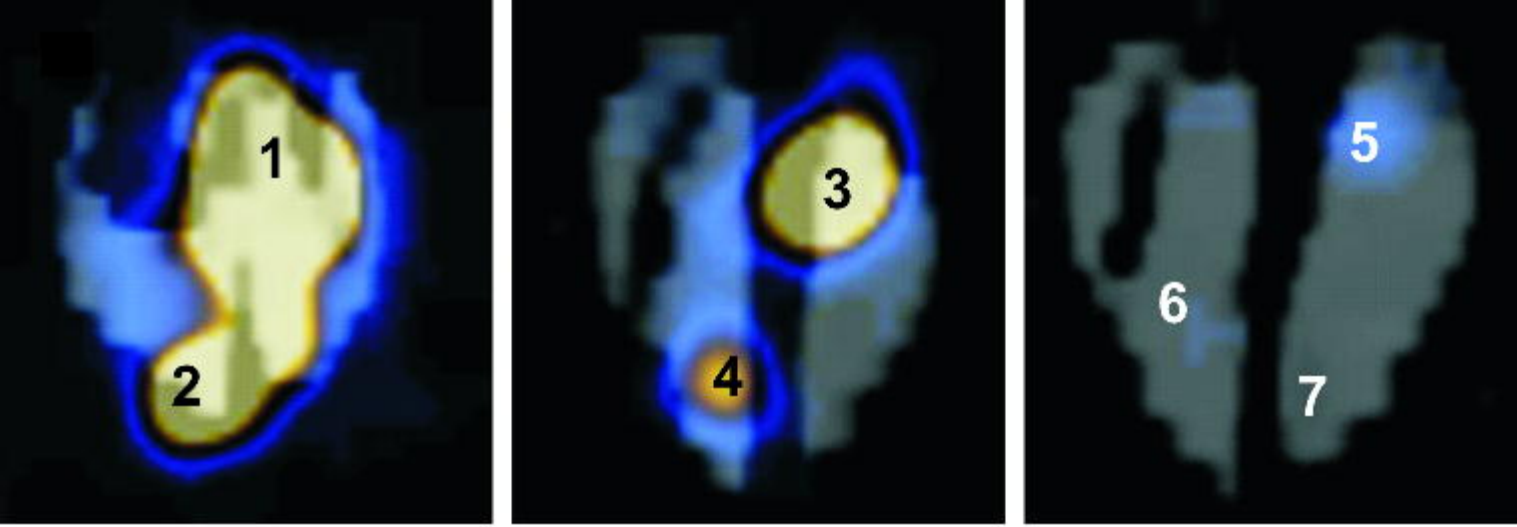

Figure 3

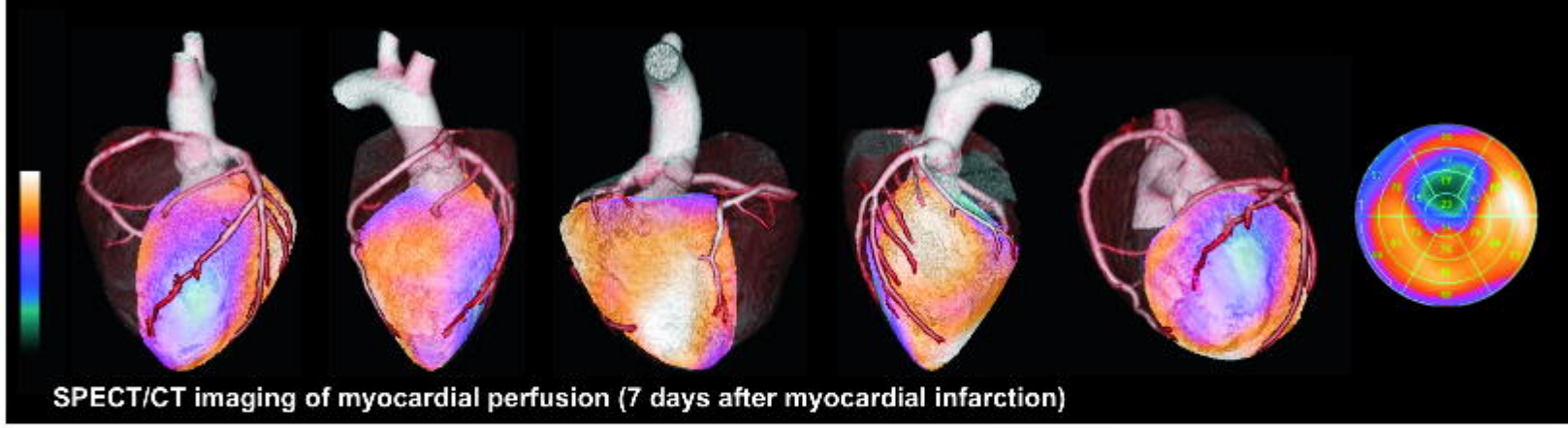

SPECT/CT imaging of myocardial perfusion (7 days after myocardial infarction)

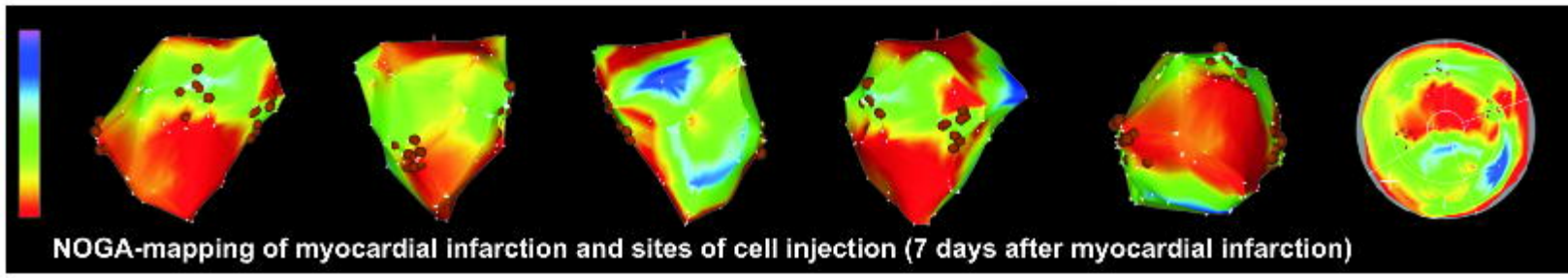

NOGA-mapping of myocardial infarction and sites of cell injection (7 days after myocardial infarction)

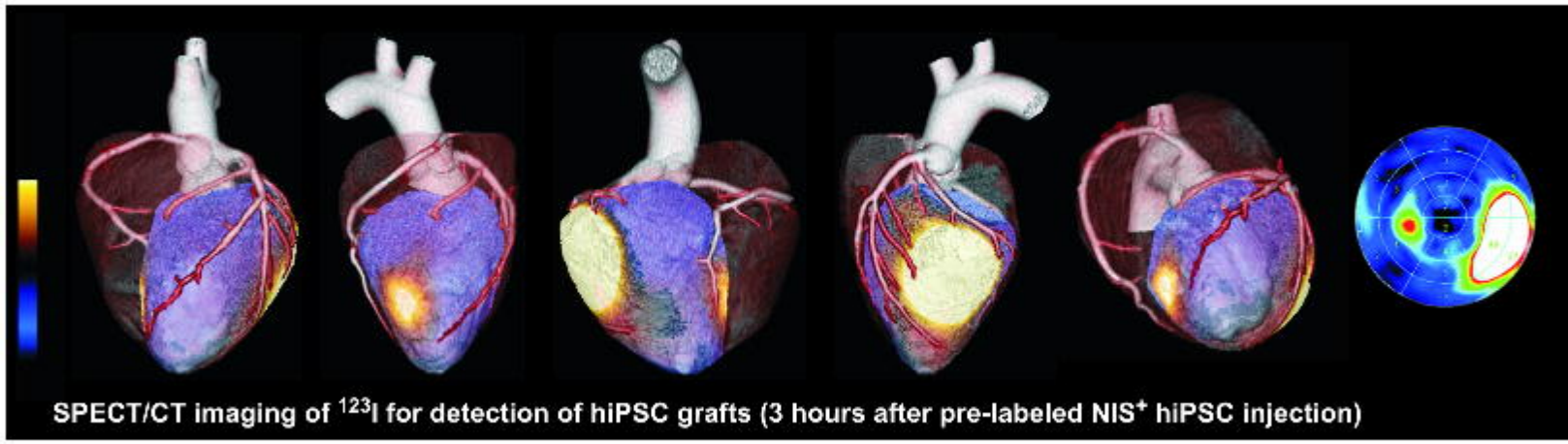

SPECT/CT imaging of ^{123}I for detection of hiPSC grafts (3 hours after pre-labeled NIS^{+} hiPSC injection)

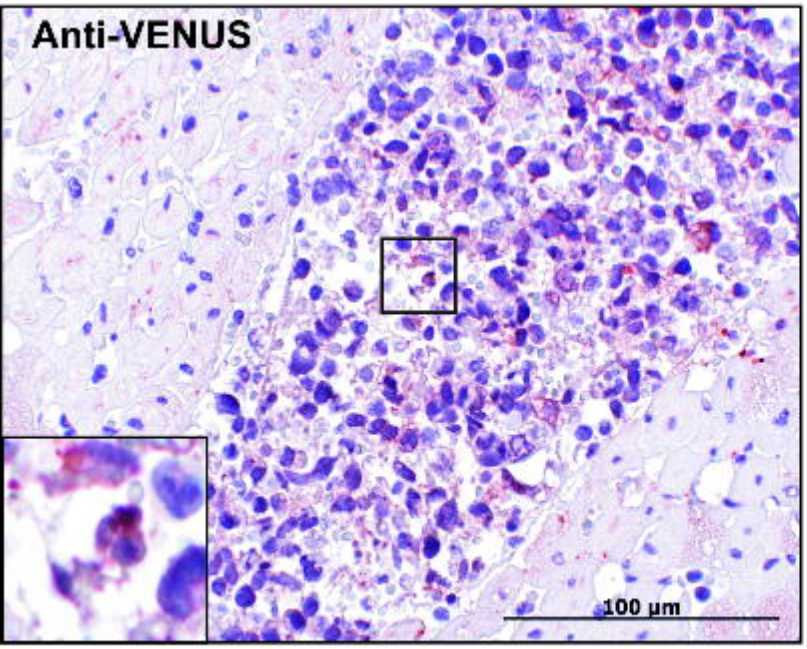

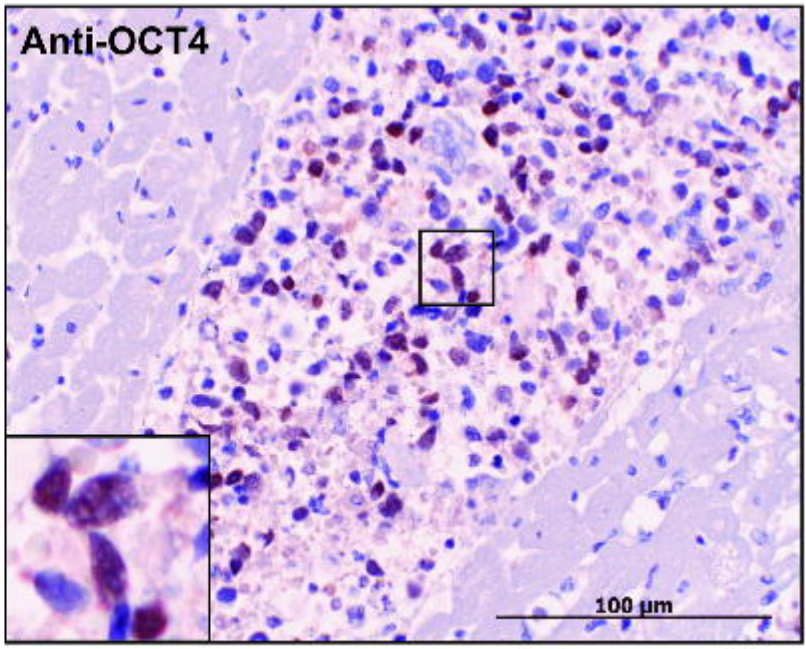

Figure 4

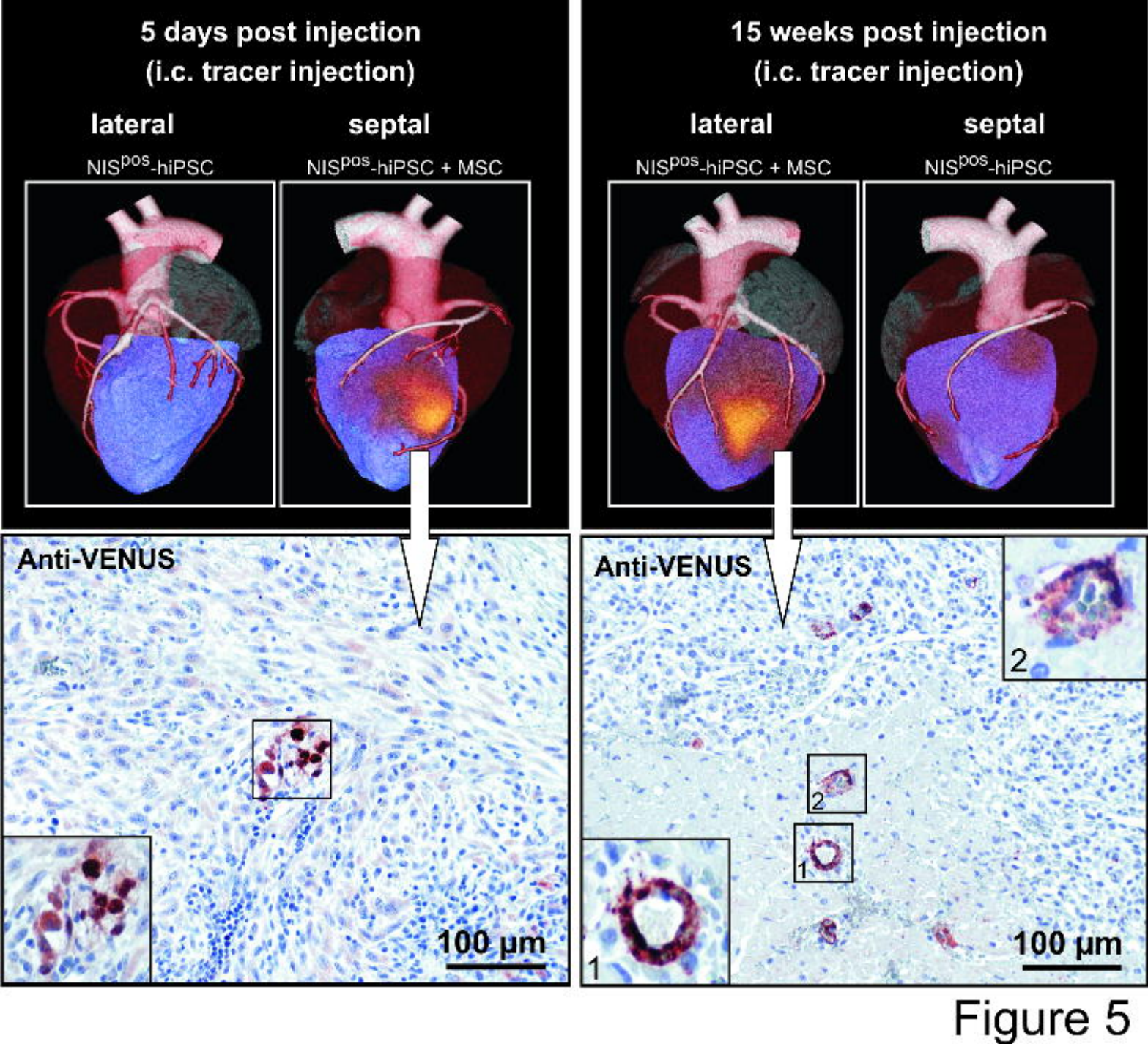
5 days post injection
(i.c. tracer injection)
lateral
septal
NIS^pos-hiPSC
NIS^pos-hiPSC + MSC
15 weeks post injection
(i.c. tracer injection)
lateral
septal
NIS^pos-hiPSC + MSC
NIS^pos-hiPSC
Anti-VENUS
100 µm
Anti-VENUS
1
2
100 µm

Figure 5